International Journal of Mechanical, Industrial and Aerospace Sciences
ISSN: 2517-9950
Vol:12, No:6, 2018

Cellulose Nanocrystals Suspensions as Water-Based Lubricants for Slurry Pump Gland Seals

Mohammad Javad Shariatzadeh, Dana Grecov

***Abstract*—**The tribological tests were performed on a new tribometer, in order to measure the coefficient of friction of a gland seal packing material on stainless steel shafts in presence of Cellulose Nanocrystal (CNC) suspension as a sustainable, environmentally friendly, water-based lubricant. To simulate the real situation from the slurry pumps, silica sands were used as slurry particles. The surface profiles after tests were measured by interferometer microscope to characterize the surface wear. Moreover, the coefficient of friction and surface wear were measured between stainless steel shaft and chrome steel ball to investigate the tribological effects of CNC in boundary lubrication region.

Alignment of nanoparticles in the CNC suspensions are the main reason for friction and wear reduction. The homogeneous concentrated suspensions showed fingerprint patterns of a chiral nematic liquid crystal. These properties made CNC a very good lubricant additive in water.

***Keywords*—**Gland seal, lubricant additives, nanocrystalline cellulose, water-based lubricants.

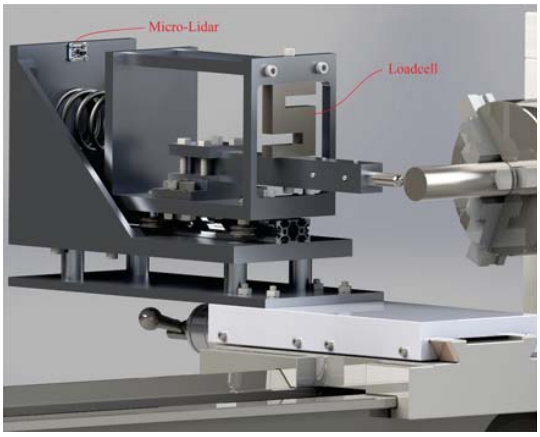

Fig. 1 Schematic of the circular shaft Tribometer

I. Introduction

THE friction on circular shafts is an important concern for slurry pumps. Slurry pump gland seals are particularly used in mineral processing pumps to avoid entering the pumped fluid (slurry) to the external environment [1]. The slurry particles entrained in the gap of a gland seal create a lubricated abrasive wear contact mechanism and is analogous to the wear of plain bearing journals. If the slurry is hazardous, the seal failure may create an unsafe workplace. To reduce the seal failure rate, a high-performance lubricant is needed, which in addition to reduce the friction and remove wear particles, is free of harmful additives or chemicals [2]. Currently, water is used to lubricate the gland seal packing materials. It is environmentally friendly, inexpensive, readily available, non-flammable and has high thermal conductivity [3]. However, due to its low viscosity, corrosive properties, low boiling point and high freezing point, the water is unacceptable for most tribological applications [4], [5].

Additives are used to reduce shortcomings and improve the water properties [6]. With the development of nanotechnology and the deepening understanding of particularity of functional nano-materials, nanoparticles used as additives show unique physical and chemical properties and have a broad application prospect in lubrication [7]. Cellulose nanocrystal (CNC) is a nanomaterial with unique properties and one of the abundant, sustainable, and environmentally friendly cellulose derivatives. It is typically extracted from cellulosic biomass using strong acid hydrolysis. The hydrolysis conditions and cellulose source affect the surface chemistry and particle size of isolated CNC particles [8]. The elimination of amorphous domain in cellulosic materials made CNC a highly crystalline material. The specific surface area of CNC can reach up to several hundred square meters per gram, resulting in a large number of nanoparticle interactions as well as outstanding fluid properties at low concentrations [9]. Very good mechanical, reinforcement and other properties make CNC the ideal materials for processing polymer nanocomposites. CNC is also used as the rheology modifier in polymers, paint, cosmetics and pharmaceutical products [10]. CNC suspensions present thixotropic shear thinning behavior that makes them effective rheological modifier to improve the rheological performance of water-based drilling fluids [9].

Mohammad Javad Shariatzadeh and Dana Grecov are with the Department of Mechanical Engineering, University of British Columbia, Vancouver, BC V6T 1Z4 Canada (e-mail: shariatzadeh@alumni.ubc.ca).

II. Experimental Method

A new tribometer, measuring the friction of cylindrical shafts has been designed and built.

The circular shaft is gripped between a lathe chucks and rotated by an electrical motor at different rotational speeds. The friction between shaft surface and pin enforces a beam to bend. A load cell with the accuracy of 0.01 N, is stretched due to the beam bending and produces a voltage. By calibrating the output voltage and force on the tip of the pin we can measure the friction force. The radial and axial positions of the tribometer are controlled by the lathe carriage with a precision of 0.001 mm in the radial direction and 0.01 mm in the axial direction.

The normal force is produced by a stiff spring which can exert a maximum normal force of 800 N. By measuring the radial movement of carriage which is equal to the compressed

length of the spring, the spring force can be calculated. There is a linear relation between the normal force and the springs length. A Micro-LIDAR distance sensor with an error of 0.05 mm is used (Fig. 1) to measure the spring length. Data from the load cell and lidar are collected by an Arduino Uno board and transferred to the computer. Real-time curves of normal force (lidar data), friction force (load cell data) and coefficient of friction (ratio of friction force to normal force) are plotted by a developed GUI.

Tribological studies of cylindrical shafts were performed at room temperature with the tribometer. The stainless steel shaft with a diameter of 2 inches was initially polished to get a very smooth surface with the roughness of 0.5 microns. Then, the sample was cleaned by sonication in isopropanol alcohol to remove any organic contaminants that may have been left from the machining and polishing operations performed during sample preparation. The counterpart was graphite fiber gland packing with 10x10 mm cross-section. The normal force during tests was 50 N at a rotational speed of 130 rpm.

CNC powder was purchased from CelluForce Inc. with the particle size of $1 - 50\mu m$ and sulfur content of 0.86-0.89%.CNC powder was added to water to make aqueous suspensions with concentrations of 2 wt.%, 3 wt.%, and 4 wt.%. To prepare the CNC aqueous suspensions, Ultrasonic processor model VCX-130 (Sonics & Materials Inc.) with a 6 mm probe was used to apply ultrasound energy (1000 Joules per gram of CNC) to suspensions in order to disperse the CNC particles. For tribological tests, the suspensions were used as lubricants during experiments with the flow rate of 1.25 ml per minute. Before tribological tests, the viscosity of suspensions has been measured as a key parameter of a lubricant. Although many articles discussed viscosity of CNC [11], [12], the viscosity in high shear rates has not been reported. In tribological tests, due to the small gap between contact surfaces and high relative rotational speed, usually, the shear rates are very high. The rheological measurements for low shear rates (0.1-500 $s^{-}1$) were performed on a Kinexus Rheometer (Malvern Instruments Ltd., UK) using a cone and plate geometry (2 cone angle, 60 mm diameter). For high shear rates (0.1 to 7000 $s^{-}1$) the measurements were performed on a microfluidic rheometer with a niddle radius of 0.545 mm and length of 332.8 mm.

In the real situation, slurry particles enter the gap between shaft and gland seal packing and produce a complex tribological environment which causes friction increasing, heat generation, lubricant loss and raise of wear rate. The particle size distribution strongly depends on the transported mineral type. Generally, the specific wear rate increases with the particle size [13]. The experimental particle distribution size included more than 80% particles from 30-40 mesh. Washed and dried silica sands were used as slurry particles and purchased from VWR ANALYTICAL Company. Particles were added to the experiment at the rate of 0.6 gram per minute as shown in Fig. 2.

To estimate the wear rate after the tests, we measured the surface roughness by an interferometer microscope and calculated the root mean square (RMS) roughness from the following equation

Fig. 2 Experimental setup with packing material and sands

$$RMS = \sqrt{\frac{\Sigma(Y_i - \bar{Y})^2}{N-1}} \quad (1)$$

where, Y is the height of each point on the surface from a certain level and N is the number of points on the surface where their heights are measured by an interferometer microscope. In our experiments, N is 640.

III. Results and Discussion

For each lubricant, three sets of experiments were performed and the following results are averaged of all sets. The coefficient of friction versus time between stainless steel shaft and packing material is shown in Fig. (3). The steady-state coefficients of friction for water, CNC2 wt.%, CNC 3 wt.% and, CNC 4 wt.% are 0.36, 0.30, 0.27, and 0.31 respectively.

The surface roughness after experiments is changed because of abrasive wear caused by sands. The surface profiles are captured by interferometer microscope on 10 different regions of the surfaces. A sample profile for each case is shown in Fig. 4. The average surface roughness for water, CNC 2 wt.%, CNC 3 wt.% and, CNC 4 wt.% is 1.45 μm, 0.61 μm, 0.19 μm, and 0.68 μm respectively.

Elastohydrodynamic lubrication (EHL) occurred in the friction tests because the elastic deformation of packing material plays a fundamental role. As it can be seen from Fig. 3, the coefficient of friction does not change significantly, because deformation of the packing material and presence of abrasive sands do not allow the lubricant to make a thick film in the contact region to support the load and pulls the surfaces apart. A 25% friction reduction was obtained for CNC 3 wt.% compared to water. Nevertheless, the wear rate reduced significantly for CNC. The surface roughness in case of lubrication with CNC 3 wt.% was reduced more than 7.5 times compare to lubrication with water which could lead to an important increase in the shaft life cycle.

To investigate further the lubrication effect of CNC addition to water, the same experiment was conducted between a 1-inch stainless steel shaft and a chrome steel ball with the diameter of 6 mm. Results of the coefficient of frictions are shown in

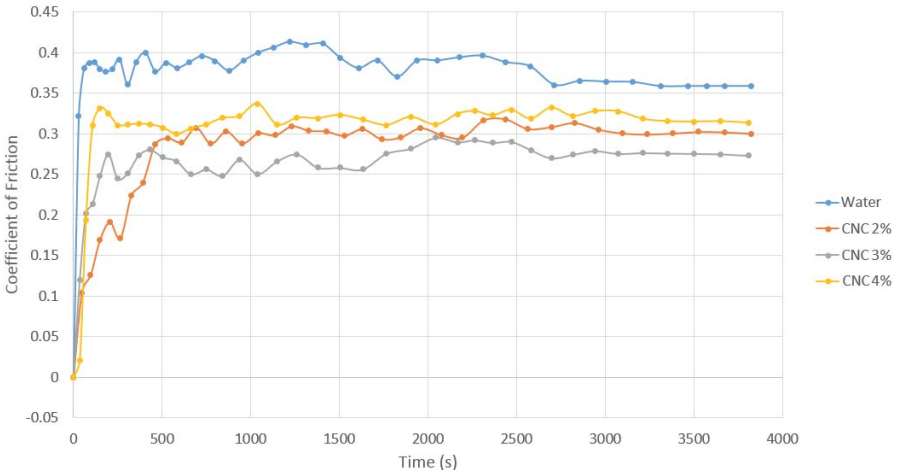

Fig. 3 Coefficient of friction between stainless steel and packing material in presents of different lubricants

TABLE I
SCAR DEPTH AND WIDTH MEASURED BY INTERFROMETER

	Water	CNC 2 wt.%	CNC 3 wt.%	CNC 4 wt.%
Scar depth	$67.2\mu m$	$38.1\mu m$	$49.4\mu m$	$61.4\mu m$
Scar width	$1.78mm$	$0.98mm$	$1.15mm$	$1.32mm$

Fig. 5. After passing the static friction region and experiencing high friction force, the coefficient of friction decreased until it reached a steady state. The steady state coefficient of friction for water, CNC 2 wt.%, CNC 3 wt.% and, CNC 4 wt.% is 0.33, 0.11, 0.15, and 0.19 respectively which shows that CNC can reduce the friction by a factor of 3.

Also, the results of wear reduction between stainless steel and chrome steel ball show that CNC addition to water can reduce the wear rate. The depth and width of scars are measured by interferometer microscope on 10 different regions and the averaged values are shown in Table I. A sample picture of a scar for CNC 3 wt.% is shown in Fig. 6.

The improvement of the coefficient of friction and wear by CNC addition to water is due mainly to the orientation and alignment of CNC particles. Cellulose chains assemble in an ordered structure due to hydrogen bonding formed by OH groups on their surfaces [14]. The abundance of OH groups on the surface of cellulose favors the formation of hydrogen bonding, causing the cellulose chains to assemble in highly ordered structures [14]. When sulfuric acid is used as the hydrolyzing agent, it also chemically reacts with the surface hydroxyl groups of CNC to yield negatively charged sulfate groups that promote a perfectly uniform dispersion of the whiskers in water via electrostatic repulsions [15]. Increasing concentration of the solid phase causes the CNC to adopt configurations that minimize the existing electrostatic interactions. Indeed, homogeneous concentrated suspensions self-organize into a liquid crystalline structure. This self-organization phenomenon was revealed by the appearance of fingerprint patterns obtained from suspensions observed by a Polarized Optical Microscope, indicative of a chiral-nematic ordering [16]. A sample image of CNC fingerprint is shown in Figure (7). Shear rate can change the structure of CNC and liquid crystals arrangement of nanoparticles. Figure (8) depicts the viscosity profile of CNC suspensions versus shear rate. The viscosity decrease is significant for all the concentrations and the samples show the behavior of liquid crystalline systems [17]. Starting from chiral nematic ordered domains in the system, the suspension goes through the shear thinning region, where viscosity decreases due to deformation and realignment of chiral nematic domains. By increasing the shear rate, these domains become aligned along the shear direction and eventually break down. Due to the increase in shear rate, the bonds are broken, liquid crystal domains are no longer present in the suspension and the individual CNC rods essentially align themselves in the direction of shear rate [12].

IV. CONCLUSION

CNC as a sustainable and environmentally friendly cellulose derivatives exhibit remarkable improvement of coefficient of friction and wear when added to water. The friction coefficient between stainless steel shaft and chrome steel ball in presence of CNC with 2 wt.% as a water-based lubricant is 0.11 which is approximately 1/3 of the friction coefficient of water. In addition to friction reduction, CNC reduced the wear depth and width by 50%.

CNC suspension can be used as a lubricant in slurry pumps gland seal. CNC with 3 wt.% shows the best result of coefficient of friction in presence of abrasive sands. The surface roughness in case of lubrication with CNC 3 wt.% reduced more than 7.5 times compare to lubrication with water which can increase the life cycle of shaft and gland seal packing material.

The beneficial properties of CNC suspensions are mainly caused by orientation and alignment of its nanoparticles. The nanoparticles orient along the shear direction in the contact region between the two sliding surfaces, hence decreasing the friction coefficient and the wear between the sliding surfaces.

These results suggest a good potential for the application of CNC as a water lubricating additive to reduce friction and surface wear.

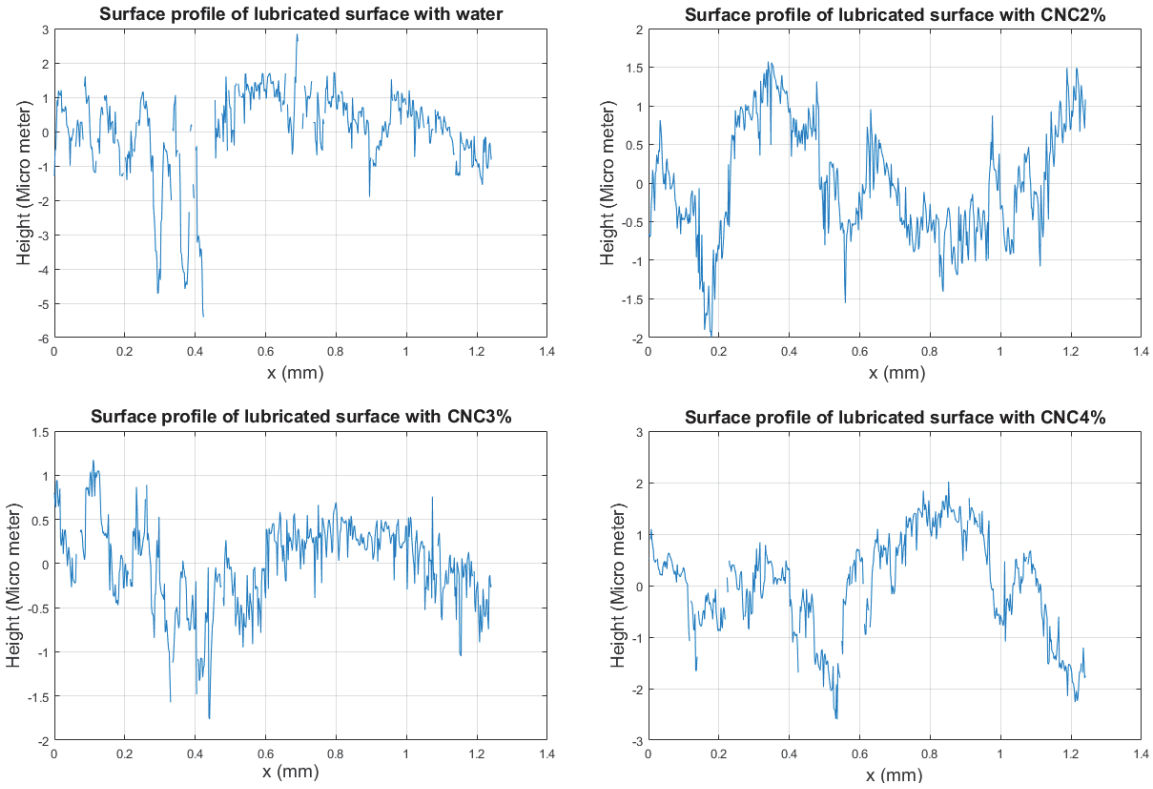

Fig. 4 Wear profile of lubricated surfaces with different lubricants

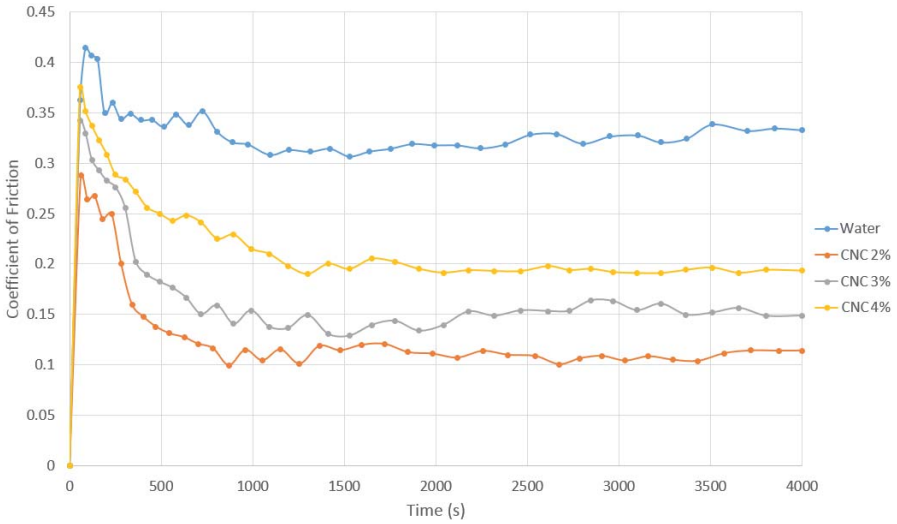

Fig. 5 Coefficient of friction between stainless steel and chrome steel ball in presents of different lubricants

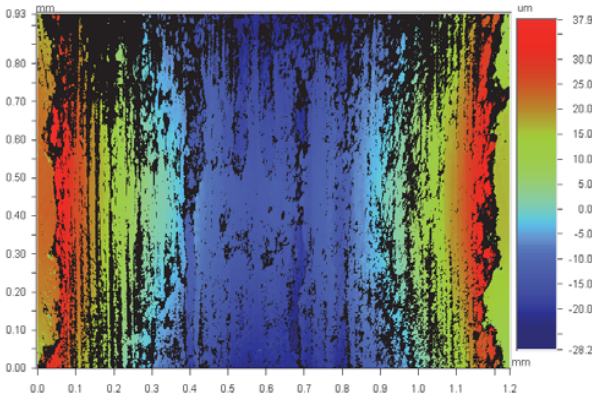

Fig. 6 Profile of a scar on the surface of 1-inch stainless steel shaft lubricated with CNC 3wt.%

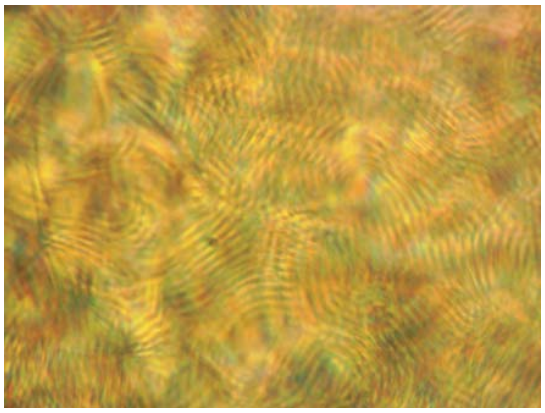

Fig. 7 Fingerprint patterns obtained from CNC 4 wt.% suspension observed by a Polarized Optical Microscope, indicative of a chiral-nematic ordering. The horizontal length of image is 350 μm

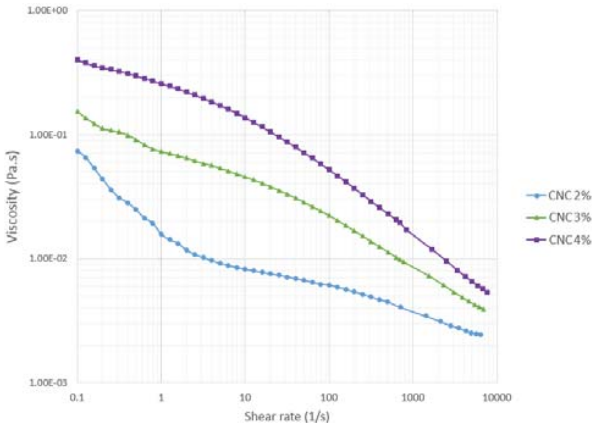

Fig. 8 viscosity profile of CNC suspensions versus shear rate

References

[1] N. Ridgway, C. Colby, B. ONeill, Slurry pump gland seal wear, Tribology International 42 (11) (2009) 1715–1721.
[2] B. Khorramian, G. Iyer, S. Kodali, P. Natarajan, R. Tupil, Review of antiwear additives for crankcase oils, Wear 169 (1) (1993) 87–95.
[3] M. W. Sulek, T. Wasilewski, Tribological properties of aqueous solutions of alkyl polyglucosides, Wear 260 (1) (2006) 193–204.
[4] A. Tomala, A. Karpinska, W. Werner, A. Olver, H. Störi, Tribological properties of additives for water-based lubricants, Wear 269 (11) (2010) 804–810.
[5] H. Lei, W. Guan, J. Luo, Tribological behavior of fullerene–styrene sulfonic acid copolymer as water-based lubricant additive, Wear 252 (3) (2002) 345–350.
[6] R. M. Gresham, The mysterious world of mwf additives, Tribology and Lubrication Technology 62 (9) (2006) 30.
[7] Y. Bao, J. Sun, L. Kong, Effects of nano-sio 2 as water-based lubricant additive on surface qualities of strips after hot rolling, Tribology International 114 (2017) 257–263.
[8] X. M. Dong, J.-F. Revol, D. G. Gray, Effect of microcrystallite preparation conditions on the formation of colloid crystals of cellulose, Cellulose 5 (1) (1998) 19–32.
[9] M.-C. Li, Q. Wu, K. Song, C. F. De Hoop, S. Lee, Y. Qing, Y. Wu, Cellulose nanocrystals and polyanionic cellulose as additives in bentonite water-based drilling fluids: rheological modeling and filtration mechanisms, Industrial & Engineering Chemistry Research 55 (1) (2015) 133–143.
[10] Y. C. Ching, M. E. Ali, L. C. Abdullah, K. W. Choo, Y. C. Kuan, S. J. Julaihi, C. H. Chuah, N.-S. Liou, Rheological properties of cellulose nanocrystal-embedded polymer composites: a review, Cellulose 23 (2) (2016) 1011–1030.
[11] M. A. Hubbe, P. Tayeb, M. Joyce, P. Tyagi, M. Kehoe, K. Dimic-Misic, L. Pal, Rheology of nanocellulose-rich aqueous suspensions: A review, BioResources 12 (4) (2017) 9556–9661.
[12] S. Shafiei-Sabet, W. Y. Hamad, S. G. Hatzikiriakos, Rheology of nanocrystalline cellulose aqueous suspensions, Langmuir 28 (49) (2012) 17124–17133.
[13] A. Misra, I. Finnie, On the size effect in abrasive and erosive wear, Wear 65 (3) (1981) 359–373.
[14] C. Salas, T. Nypelö, C. Rodriguez-Abreu, C. Carrillo, O. J. Rojas, Nanocellulose properties and applications in colloids and interfaces, Current Opinion in Colloid & Interface Science 19 (5) (2014) 383–396.
[15] J.-F. Revol, H. Bradford, J. Giasson, R. Marchessault, D. Gray, Helicoidal self-ordering of cellulose microfibrils in aqueous suspension, International journal of biological macromolecules 14 (3) (1992) 170–172.
[16] Y. Habibi, L. A. Lucia, O. J. Rojas, Cellulose nanocrystals: chemistry, self-assembly, and applications, Chemical reviews 110 (6) (2010) 3479–3500.
[17] J. J. Magda, S. G. Baek, K. DeVries, R. Larson, Shear flows of liquid crystal polymers: measurements of the second normal stress difference and the doi molecular theory, Macromolecules 24 (15) (1991) 4460–4468.